# DNA-mediated Step-growth Polymerization of Bottlebrush Macromonomers

Xueguang Lu,[†,#] Hailin Fu,[‡,§,#] Kuo-Chih Shih,[‡] Fei Jia,[†] Yehui Sun,[†] Dali Wang,[†] Yuyan Wang[†], Stephen Ekatan,[‡,§] Mu-Ping Nieh,[‡,#,*] Yao Lin,[‡,§,*] and Ke Zhang[†,*]

[†]Department of Chemistry and Chemical Biology, Northeastern University, Boston, Massachusetts 02115, United States

[‡]Polymer Program, Institute of Materials Science, University of Connecticut, Storrs, Connecticut 06269, United States

[§]Department of Chemistry, University of Connecticut, Storrs, Connecticut 06269, United States

[#]Department of Chemical and Biomolecular Engineering, University of Connecticut, Storrs, Connecticut 06269, United States

*Supporting Information Placeholder*

**ABSTRACT:** Herein, we report the DNA-mediated self-assembly of bivalent bottlebrush polymers, a process akin to the step-growth polymerization of small molecule monomers. In these "condensation reactions", the polymer serves as a steric guide to limit DNA hybridization in a fixed direction, while the DNA serves as a functional group-equivalent, connecting complementary brushes to form well-defined, one-dimensional nanostructures. The polymerization was studied using spectroscopy, microscopy, and scattering techniques, and was modeled numerically. The model made predictions of the degree of polymerization and size distribution of the assembled products, and suggested the potential for branching at hybridization junctions, all of which were confirmed experimentally. This study serves as a theoretical basis for the polymer-assembly approach which has the potential to open up new possibilities for suprapolymers with controlled architecture, macromonomer sequence, and end-group functionalities.

In nature, proteins non-covalently interact with each other to form extremely well-defined structures.[1,2] There has long been an interest in replicating nature's ability to prepare complex mesoscale structures using synthetic materials.[3–7] DNA is an ideal tool for building pre-defined mesoscale structures from nanoscale building blocks, owing to the highly predictable, programmable, and precise base-pairing, both canonical and non-canonical.[8,9] Since the 1990s, advances in DNA nanotechnology have established the fundamental rules for directional DNA assembly, which involves rigidified DNA building blocks.[10,11]

Currently, two chemically and conceptually distinct pathways are employed to provide the necessary rigidity to the DNA building blocks. In one approach, rigidity is derived from multiple strand crossovers stabilized by hybridization, which create a conformationally restricted DNA scaffold.[12–14] To date, a vast range of highly complex two- and three-dimensional structures have been reported using this method.[15–20] However, while enjoying near-complete freedom in structural diversity, this approach is limited to a chemical composition of pure nucleic acid. In the second approach, a rigid, non-nucleic acid nanoparticle (inorganic or organic) is employed as a template to organize functionalized DNA strands in a surface-normal orientation.[21–25] This method opens up a great deal of compositional diversity, but the accessible structures are limited to the repeating patterns of crystal lattices. Directional assembly of these spherical building blocks to even the simplest form, one-dimensional structures (i.e., lines), represents a significant challenge, because spherical particles uniformly interact across their surfaces, leading to omnidirectional, three-dimensional growth. Therefore, an opportunity exists to use DNA as a functional group equivalent to create a series of limited-valency macromonomers for topologically defined supramolecular assembly, which will accomplish both structural and compositional diversities.

**Scheme 1.** (A) Synthesis of DNA-brush macromonomer. (B) DNA sequence design.

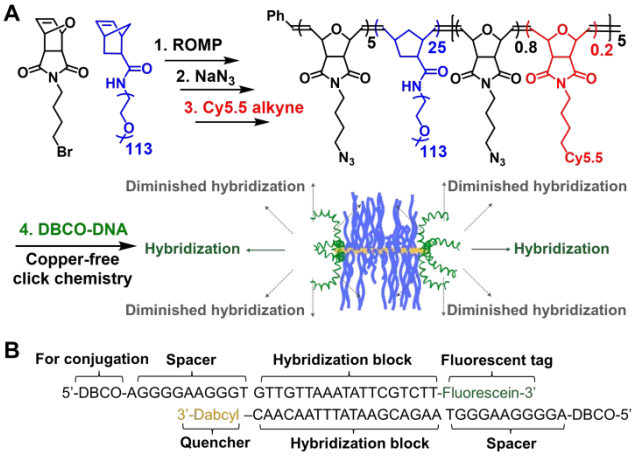


A small number of methods have been reported to control the bonding directions of DNA-containing building blocks. Mirkin et al. reported a bivalent DNA-protein conjugate, of which the DNA strands were attached to two opposite surfaces.[26,27] A similar approach was also reported by Gang et al., who utilized the rigid octahedra DNA frame to direct DNA hybridization.[28] Our group first reported a class of DNA-brush

polymer conjugate that restricted the bonding directionality of spherical building blocks to one dimension.[29] These conjugates consist of a bottlebrush polymer with DNA strands tethered at both ends of the polymer backbone. The sterically congested polymer create an entropic force that pre-orients the embedded DNA strands and allows the conjugate to adopt a unidirectional bonding character.[30–32] Despite the successful proof of concept, there still lacks an understanding of the kinetics for the assembly process, which prevents any means of predicting the assembled structures, including the chain length, polydispersity, and branching. Herein, we report the first two-monomer (AA+BB) reaction system based on DNA-brush polymer conjugates, for which we generate a numerical model with predictive capabilities.

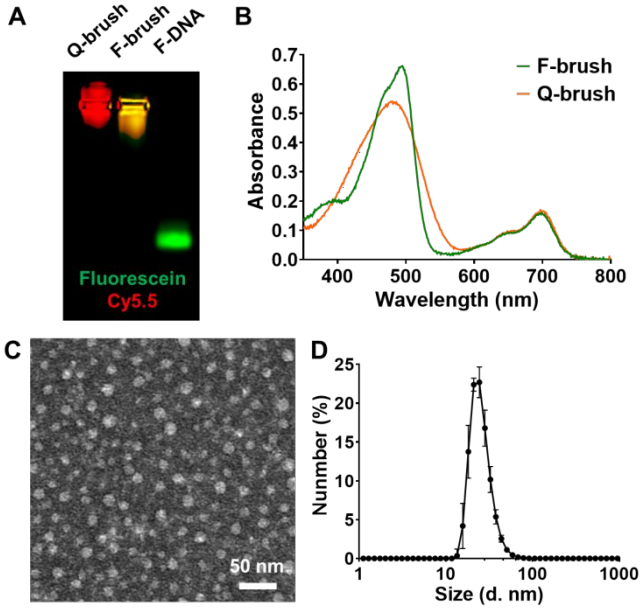


**Figure 1.** (A) Gel electrophoresis of F-brush, Q-brush, and F-DNA. The emissions from fluorescein and Cy5.5 are colored green and red, respectively. (B) UV-Vis spectra of F- and Q-brushes. (C) Negatively stained TEM image and (D) number-average hydrodynamic size distribution of the F-brush.

A pair of macromonomers with mutually complementary sequences (AA+BB) were synthesized to mimic the typical bi-functional monomers in step-growth polymerization (Scheme 1A). The brush polymer was synthesized by one-pot, sequential ring opening metathesis polymerization (ROMP) of norbornyl-bromide (N-Br) and norbornyl polyethylene glycol (N-$PEG_{5k}$, $M_n$ = 5 kDa, PDI = 1.05), to yield a tri-block copolymer $p(N\text{-}Br)_5$-*b*-$p(PEG5k)_{25}$-*b*-$p(N\text{-}Br)_5$. The targeted five N-Br units per block would ensure >99.3% of all polymers to end up with at least one N-Br group under ideal living polymerization conditions.[33,34] The polymer was then reacted with sodium azide to yield $p(N\text{-}N_3)_5$-*b*-$p(PEG5k)_{25}$-*b*-$p(N\text{-}N_3)_5$. Gel permeation chromatography (GPC) shows that triblock brush polymer has a number-average molecular weight ($M_n$) of 128 kDa and narrow molecular weight distribution (PDI = 1.1, Figure S1). Infrared spectroscopy shows characteristic vibration of the azide groups at ~2094 $cm^{-1}$ (Figure S2). Before DNA conjugation, the brush polymer was labeled with a cyanine 5.5 (Cy5.5) tag through copper-catalyzed click chemistry (Cy5.5:polymer = 1:1 mol:mol) to enable accurate quantification.

The remaining terminal azide groups were used to conjuguate with DNA strands modified with dibenzylcyclooctane (DBCO). The two complementary DNA strands were labeled with either fluorescein (F-DNA) or dabcyl (a fluorescence quencher, Q-DNA) at the 3' (Scheme 1B). The DNA strands were conjugated to the brush polymer via copper-free click chemistry, and unreacted DNA was removed by aqueous GPC to yield F-brush and Q-brush (Figure S3). The numbers of F-DNA and Q-DNA strands per brush were calculated to be ~10 for both F- and Q-brushes by peak integration of the GPC chromatograms of reaction mixture at 260 nm. Multiplex agarose gel electrophoresis showed emissions from both fluorescein (green) of the DNA and Cy5.5 (red) of the polymer as high molecular weight bands where expected (Figure 1A). Note that the Q-brush only shows Cy5.5 emission because the dabcyl-labeled DNA strand is not fluorescent. UV-Vis spectra of the two brushes showed characteristic absorptions for dabcyl, fluorescein, and Cy5.5 (Figure 1B and S4). These DNA-brush conjugates exhibit a circular shape with a diameter of 11.0±1.7 nm as determined by transmission electron microscopy (TEM, Figure 1C), which is indicative of a spheroidal or discoidal morpology. The TEM result is consistent with dynamic light scattering (DLS) measurements, which show a number-average hydrodynamic diameter of 17.8±5.1 nm (Figure 1D). Collectively, these results confirm the successful synthesis of a pair of mutually reactive macromonomers.

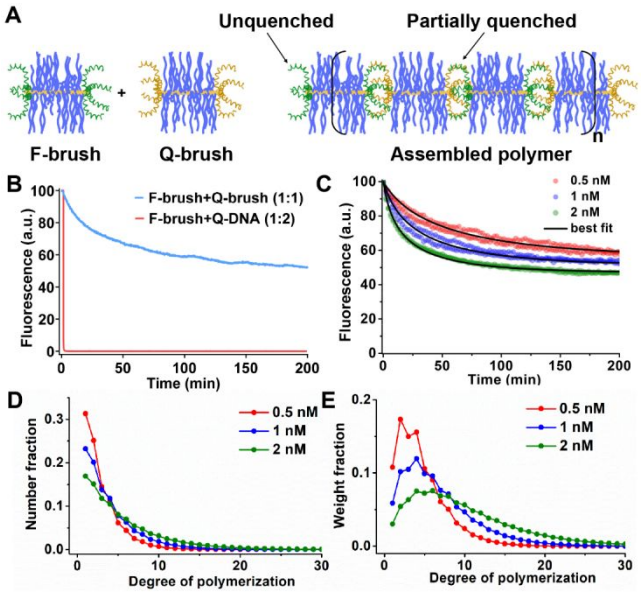


**Figure 2.** (A) Schematics of the brush polymer self-assembly. (B) Hybridization kinetics of F-brush with Q-brush or Q-DNA. (C) Model-fitting of the polymerization kinetics at different monomer concentrations. (D-E) Predicted number- and weight-based size distributions by the kinetic model.

The self-assembly kinetics can be obtained by monitoring fluorescence as a function of time. We first tested the accessibility of the F-DNA embedded in the F-brush to free Q-DNA. Upon addition of Q-DNA, fluorescence signals immediately dropped and reached equilibrium after ~2 min (Figure 2B), indicating rapid hybridization and little steric hindrance. When F- and Q-brushes were mixed in 1:1 molar ratio (concentration of each brush = 1 nM), the fluorescence intensity slowly decreased over time (Figure 2B), suggesting that the steric hindrance between the two reacting brushes is much greater than that between a brush and a free DNA.

In order for the two brushes to be brought into close proximity, there would be an increase in PEG density and a decrease in the translational freedom of the macromonomers. The entropic penalty may be manifested in a decrease in the binding affinity between the two complementary DNA.[35] Indeed, for the assembly of F- and Q-brushes, the fluorescence level remained relatively high (~52% of F-DNA unquenched) even after prolonged reaction times (180 min), suggesting that the reaction is reversible. However, the reaction conversion cannot be directly interpreted from the percentage of quenched DNA because the F-DNA strands on each side of the brush polymer do not necessarily all hybridize with the Q-DNA, leading to incomplete quenching even when all the brushes undergo polymerization. Therefore, to numerically model the polymerization kinetics, a concentration-dependent polymerization study was performed.[36,37] Three concentrations of F-brush (0.5, 1, and 2 nM) were mixed in 1:1 ratio with the Q-brush and the polymerization kinetics were recorded by fluorescence spectroscopy. The data were globally fitted by numerical methods using a reversible step-growth polymerization model (eq. 1), where i-mers ($M_i$) and j-mers ($M_j$) can reversibly associate and dissociate with rate constants $k_{on}$ and $k_{off}$, *respectively* (the detailed differential equations are shown in SI). In the fitting, we hypothesize that the normalized fluorescence is proportional to the sum of the number of monomers, oligomers, and a fraction (f) of the connecting bonds (eq 2).

$$M_i + M_j \underset{k_{off}}{\overset{k_{on}}{\rightleftharpoons}} M_{i+j} \qquad 1 < i + j \leq N_{\max} \tag{1}$$

$$\text{Normalized Fluorescence} = \frac{100}{[M]_0} * \left( \sum_{i=1}^{N_{max}} [M_i] + f * \sum_{i=1}^{N_{max}} (i-1) * [M_i] \right) (0 < f < 1) \tag{2}$$

where $[M]_0$ is the sum of the starting concentration of F-brush and Q-brush, $[M_i]$ is the concentration of i-mers, and $f$ is the fraction factor of the fluorescent F-DNA at the connecting bonds.

The model fits experimental profiles nicely at all concentrations tested (Figure 2C). The dissociation equilibrium constant ($k_{off}/k_{on}$) is determined to be 0.07 nM. The model predicts the number-averaged degree of polymerization ($DP_n$) for the three tested concentrations (0.5, 1, and 2 nM) to be 2.9, 3.9, and 5.6, respectively. The $f$ value is determined to be 0.35, which means 65% of fluorescence was quenched at the connecting bonds.

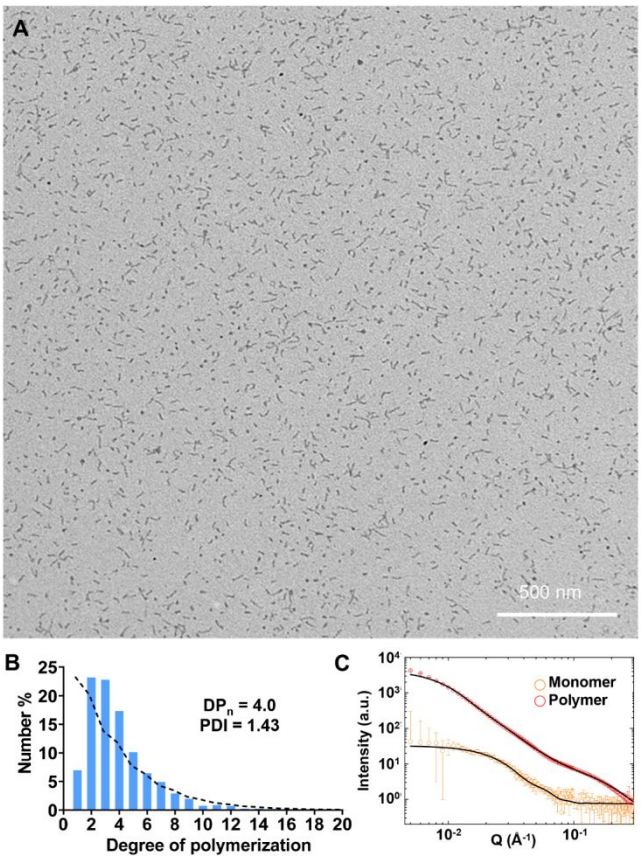


**Figure 3.** TEM image (A) and number-based polymer distribution (B) of the assembled nanostructure after mixing F-brush and Q-brush (1 nM) at 1:1 ratio. The dash line represents predicted distributions by kinetic model. (C) SAXS scattering patterns of F-brush and assembled nanostructure (1 nM).

To validate the modeling data, the assembled structures at 0.5 and 1 nM were analyzed by TEM. The brushes connected head-to-tail linearly to form rod-like structures with a cross-section diameter of ~8.8 nm and virtually no branching (<1% by number, Figures 3A, S5-6), indicating good control over the bonding directionality. The $DP_n$ (PDI ) were estimated by measuring the length/width ratio of >2000 particles to be 2.9 (1.34) at 0.5 nM, and 4.0 (1.43) at 1 nM, respectively (Figure 3B, S5, and S7), agreeing well with predicted values ($DP_n$ = 2.9, PDI = 1.56 at 0.5 nM; $DP_n$ = 3.9, PDI = 1.65 at 1 nM). The rod-like morphology was also confirmed by small angle X-ray scattering (SAXS, Figure 3C). While the scattering patterns of the F-brush suggest a discoidal morphology with a diameter of ~17 nm and a height of ~4.5 nm, the assembled structure of 1 nM shows a scattering pattern of a rod-like shape, with an degree of polymerization of ~4.1, which is consistent with the TEM and the modeling analyses. Collectively, these results suggest that the DNA-mediated self-assembly of mesoscopic polymers follows the same general rules established for small molecule polymerization.

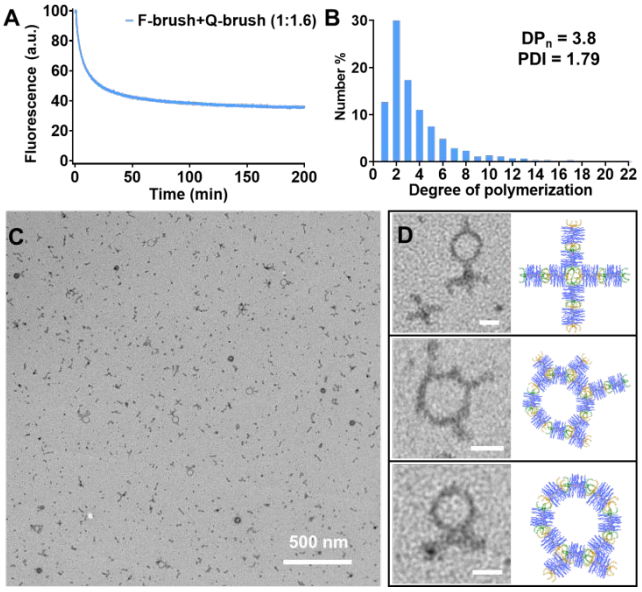


**Figure 4.** Hybridization kinetics (A), number-based polymer distribution (B), and TEM images (C and D) of assembled nanostructure after mixing F-brush and Q-brush at 1:1.6 ratio. Scale bars are 30 nm.

The modeling results confirm our hypothesis that not all DNA strands form duplexes at the connecting bonds. We were curious to know the accessibility of the remaining F-DNA at those junctions to additional Q-brushes. Therefore, we deliberately introduced a stoichiometric imbalance to the assembly system by using an excess of Q-brush (F:Q brush = 1:1.6, mol:mol, total 2.6 nM). Fluorescence monitoring showed a decrease in normalized fluorescence than the reaction at 1:1 ratio (Figure 4A), indicating more bond formation. The classic Carothers equation would predict a sharp decrease in the degree of polymerization due to the stoichiometry imbalance. Surprisingly, TEM imaging showed the formation of rod-like, branched, and cyclic structures, with a similar $DP_n$ (~3.8) but a higher PDI (1.79) compared with the reaction at 1:1 monomer ratio. One interpretation is that the excess Q-brushes hybridized to the F-DNA at the bonding junctions, deviating from the directional assembly (Figure 4C, D and S8). These results imply that the brush polymer cannot fully restrict the embedded DNA to bind to a fixed direction. Instead, the unidimensional DNA binding may be slightly more favorable over branching thermodynamically.

In summary, we studied DNA hybridization-mediated self-assembly of bottlebrush polymers into one-dimensional suprapolymers. The directionality is achieved by the steric congestion of the bottlebrush polymer, which disfavors non-linear connectivity, likely via thermodynamics. We modeled the assembly process assuming the reaction is similar to small molecule-based, reversible step-growth polymerization, which accurately predicted the length and dispersity of the assembled structures that are visualized by TEM and further characterized by SAXS. The methods developed herein should offer insights for other designer materials (including non-DNA systems that utilize hydrogen bonding, hydrophobic interactions, etc.) to be developed from the bottom up with principles borrowed from polymer chemistry.

## ASSOCIATED CONTENT

### Supporting Information

Materials, experimental procedures, instrumentation and supplemental figures. The Supporting Information is available free of charge on the ACS Publications website.

## AUTHOR INFORMATION

### Corresponding Authors

k.zhang@northeastern.edu;
yao.lin@uconn.edu;
mu-ping.nieh@uconn.edu

### Author Contributions

#X. L. and H. F. contributed equally.

### Notes

The authors declare no competing financial interests.

## ACKNOWLEDGMENT

KZ acknowledges support from the National Institute of General Medical Sciences (Award Number 1R01GM121612-01) and the National Science Foundation (CAREER Award Number 1453255). YL acknowledges support from the National Science Foundation (DMR-1809497). The authors thank Dr. Lin Yang, Life Science X-ray Scattering (LiX) at Brookhaven National Laboratory for support with SAXS measurements. The LiX beamline is jointly supported by the National Institute of General Medical Sciences (P41 GM111244) and the Department of Energy Office of Biological and Environmental Research (KP1605010), with additional support from NIH (S10 OD012331).

## REFERENCES

(1) Levitt, M.; Chothia, C. Structural Patterns in Globular Proteins. *Nature* **1976**, *261*, 552–558.
(2) Namba, K.; Caspar, D. L.; Stubbs, G. J. Computer Graphics Representation of Levels of Organization in Tobacco Mosaic Virus Structure. *Science* **1985**, *227*, 773–776.
(3) Lutz, J.; Ouchi, M.; Liu, D.; Sawamoto, M. Sequence-controlled polymers. *Science* **2013**, 341, 1238149.
(4) Holliday, B. J.; Mirkin, C. A. Strategies for the Construction of Supramolecular Compounds through Coordination Chemistry. *Angew. Chemie Int. Ed.* **2001**, *40*, 2022–2043.
(5) Cui, H.; Cheetham, A. G.; Newcomb, C. J.; Stupp, S. I. Self-Spontaneous and X-ray–Triggered Crystallization at Long Range in Assembling Filament Networks. *Science* **2010**, *327*, 555–560.
(6) Abdilla, A.; Dolinski, N. D.; De Roos, P.; Ren, J. M.; Van Der Woude, E.; Seo, S. E.; Zayas, M. S.; Lawrence, J.; Read De Alaniz, J.; Hawker, C. J. Polymer Stereocomplexation as a Scalable Platform for Nanoparticle Assembly. *J. Am. Chem. Soc.* **2020**, *142*, 1667–1672.
(7) Cui, H.; Chen, Z.; Zhong, S.; Wooley, K. L.; Pochan, D. J. Block Copolymer Assembly via Kinetic Control. *Science.* **2007**, *317* , 647–650.
(8) Storhoff, J. J.; Mirkin, C. A. Programmed Materials Synthesis with DNA. *Chem. Rev.* **1999**, *99*, 1849–1862.
(9) Record, M. T.; Mazur, S. J.; Melancon, P.; Roe, J. H.; Shaner, S. L.; Unger, L. Double Helical DNA: Conformations, Physical Properties, and Interactions with Ligands. *Annu. Rev. Biochem.* **1981**, *50*, 997–1024.
(10) Tian, Z.; Chen, C.; Allcock, H. R. Synthesis and Assembly of Novel Poly(Organophosphazene) Structures Based on Noncovalent "Host-Guest" Inclusion Complexation. *Macromolecules* **2014**, *47,* 31065–31072.
(11) Jones, M. R.; Seeman, N. C.; Mirkin, C. A. Programmable Materials and the Nature of the DNA Bond. *Science* **2015**, *347, 1260901*.
(12) Kallenbach, N. R.; Ma, R.-I.; Seeman, N. C. An Immobile Nucleic Acid Junction Constructed from Oligonucleotides. *Nature* **1983**, *305*, 829–831.
(13) Li, X.; Yang, X.; Qi, J.; Seeman, N. C. Antiparallel DNA Double Crossover Molecules as Components for Nanoconstruction. *J. Am.*

*Chem. Soc.* **1996**, *118*, 6131–6140.
(14) Zhang, H.; Wang, Y.; Zhang, H.; Liu, X.; Lee, A.; Huang, Q.; Wang, F.; Chao, J.; Liu, H.; Li, J.; Shi, J.; Zuo, X.; Wang, L.; Wang, L.; Cao, X.; Bustamante, C.; Tian, Z.; Fan, C. Programming Chain-Growth Copolymerization of DNA Hairpin Tiles for in-Vitro Hierarchical Supramolecular Organization. *Nat. Commun.* **2019**, *10*, 1–11.
(15) Chen, J.; Seeman, N. C. Synthesis from DNA of a Molecule with the Connectivity of a Cube. *Nature* **1991**, *350*, 631–633.
(16) He, Y.; Ye, T.; Su, M.; Zhang, C.; Ribbe, A. E.; Jiang, W.; Mao, C. Hierarchical Self-Assembly of DNA into Symmetric Supramolecular Polyhedra. *Nature* **2008**, *452*, 198–201.
(17) Chidchob, P.; Edwardson, T. G. W.; Serpell, C. J.; Sleiman, H. F. Synergy of Two Assembly Languages in DNA Nanostructures: Self-Assembly of Sequence-Defined Polymers on DNA Cages. *J. Am. Chem. Soc.* **2016**, *138*, 4416–4425.
(18) Douglas, S. M.; Dietz, H.; Liedl, T.; Högberg, B.; Graf, F.; Shih, W. M. Self-Assembly of DNA into Nanoscale Three-Dimensional Shapes. *Nature* **2009**, *459*, 414–418.
(19) Kuzyk, A.; Schreiber, R.; Fan, Z.; Pardatscher, G.; Roller, E. M.; Högele, A.; Simmel, F. C.; Govorov, A. O.; Liedl, T. DNA-Based Self-Assembly of Chiral Plasmonic Nanostructures with Tailored Optical Response. *Nature* **2012**, *483*, 311–314.
(20) Dong, Y.; Yang, Y. R.; Zhang, Y.; Wang, D.; Wei, X.; Banerjee, S.; Liu, Y.; Yang, Z.; Yan, H.; Liu, D. Cuboid Vesicles Formed by Frame-Guided Assembly on DNA Origami Scaffolds. *Angew. Chem. Int. Ed.* **2017**, *56*, 1586–1589.
(21) Mucic, R. C.; Storhoff, J. J.; Letsinger, R. L.; Mirkin, C. A. A DNA-Based Method for Rationally Assembling Nanoparticles into Macroscopic Materials. *Nature* **1996**, *382*, 607-609.
(22) Macfarlane, R. J.; Lee, B.; Jones, M. R.; Harris, N.; Schatz, G. C.; Mirkin, C. A. Nanoparticle Superlattice Engineering with DNA. *Science.* **2011**, *334*, 204–208.
(23) Park, S. Y.; Lytton-Jean, A. K. R.; Lee, B.; Weigand, S.; Schatz, G. C.; Mirkin, C. A. DNA-Programmable Nanoparticle Crystallization. *Nature* **2008**, *451*, 553–556.
(24) Nykypanchuk, D.; Maye, M. M.; van der Lelie, D.; Gang, O. DNA-Guided Crystallization of Colloidal Nanoparticles. *Nature* **2008**, *451*, 549–552.
(25) Dave, N.; Liu, J. Programmable Assembly of DNA-Functionalized Liposomes by DNA. *ACS Nano* **2011**, *5*, 1304–1312.
(26) McMillan, J. R.; Mirkin, C. A. DNA-Functionalized, Bivalent Proteins. *J. Am. Chem. Soc.* **2018**, *140*, 6776–6779.
(27) McMillan, J. R.; Hayes, O. G.; Remis, J. P.; Mirkin, C. A. Programming Protein Polymerization with DNA. *J. Am. Chem. Soc.* **2018**, *140*, 15950–15956.
(28) Lin, Z.; Xiong, Y.; Xiang, S.; Gang, O. Controllable Covalent-Bound Nanoarchitectures from DNA Frames. *J. Am. Chem. Soc.* **2019**, 141, 6797-6801
(29) Lu, X.; Watts, E.; Jia, F.; Tan, X.; Zhang, K. Polycondensation of Polymer Brushes via DNA Hybridization. *J. Am. Chem. Soc.* **2014**, *136*, 10214–10217.
(30) Lu, X.; Tran, T.-H. T.-H.; Jia, F.; Tan, X.; Davis, S.; Krishnan, S.; Amiji, M. M. M. M.; Zhang, K. K. Providing Oligonucleotides with Steric Selectivity by Brush-Polymer-Assisted Compaction. *J. Am. Chem. Soc.* **2015**, *137*, 12466–12469.
(31) Lu, X.; Jia, F.; Tan, X.; Wang, D.; Cao, X.; Zheng, J.; Zhang, K. Effective Antisense Gene Regulation via Noncationic, Polyethylene Glycol Brushes. *J. Am. Chem. Soc.* **2016**, *138*, 9097–9100.
(32) Jia, F.; Lu, X.; Wang, D.; Cao, X.; Tan, X.; Lu, H.; Zhang, K. Depth-Profiling the Nuclease Stability and the Gene Silencing Efficacy of Brush-Architectured Poly(Ethylene Glycol)-DNA Conjugates. *J. Am. Chem. Soc.* **2017**, *139*, 10605-10608
(33) Barbon, S. M.; Truong, N. P.; Elliott, A. G.; Cooper, M. A.; Davis, T. P.; Whittaker, M. R.; Hawker, C. J.; Anastasaki, A. Elucidating the Effect of Sequence and Degree of Polymerization on Antimicrobial Properties for Block Copolymers. *Polym. Chem.* **2020**, *11*, 84–90.
(34) Gody, G.; Zetterlund, P. B.; Perrier, S.; Harrisson, S. The Limits of Precision Monomer Placement in Chain Growth Polymerization. *Nat. Commun.* **2016**, *7*, 10514.
(35) Jia, F.; Lu, X.; Tan, X.; Wang, D.; Cao, X.; Zhang, K. Effect of PEG Architecture on the Hybridization Thermodynamics and Protein Accessibility of PEGylated Oligonucleotides. *Angew. Chem. Int. Ed.* **2017**, *56*, 1239-1243.
(36) De Greef, T.F.; Smulders, M.M.; Wolffs, M.; Schenning, A.P.; Sijbesma, R.P.; Meijer, E.W. Supramolecular polymerization. *Chem. Rev.* **2009**, *109*, 5687-5754.
(37) Liu, K.; Nie, Z.; Zhao, N.; Li, W.; Rubinstein, M.; Kumacheva, E. Step-growth polymerization of inorganic nanoparticles. *Science* **2010,** *329*, 197-200.

Insert Table of Contents artwork here